J Appl Physiol 112: 419–426, 2012.
First published November 23, 2011; doi:10.1152/japplphysiol.01172.2011.

Mechanical properties of human patellar tendon at the hierarchical levels of tendon and fibril

René B. Svensson,[1,2] Philip Hansen,[1] Tue Hassenkam,[2] Bjarki T. Haraldsson,[1] Per Aagaard,[3] Vuokko Kovanen,[4] Michael Krogsgaard,[5] Michael Kjaer,[1] and S. Peter Magnusson[1]

[1]*Faculty of Health Sciences, Institute of Sports Medicine Copenhagen, Bispebjerg Hospital & Center for Healthy Aging, University of Copenhagen, Copenhagen;* [2]*Nano-Science Center, University of Copenhagen, Copenhagen;* [3]*Institute of Sports Science and Clinical Biomechanics, University of Southern Denmark, Odense;* [5]*Department of Orthopedic Surgery, Bispebjerg Hospital, Copenhagen, Denmark; and* [4]*Biochemistry Laboratory, Department of Health Sciences, University of Jyväskylä, Jyväskylä, Finland*

Submitted 19 September 2011; accepted in final form 18 November 2011

Svensson RB, Hansen P, Hassenkam T, Haraldsson BT, Aagaard P, Kovanen V, Krogsgaard M, Kjaer M, Magnusson SP. Mechanical properties of human patellar tendon at the hierarchical levels of tendon and fibril. *J Appl Physiol* 112: 419–426, 2012. First published November 23, 2011; doi:10.1152/japplphysiol.01172.2011.—Tendons are strong hierarchical structures, but how tensile forces are transmitted between different levels remains incompletely understood. Collagen fibrils are thought to be primary determinants of whole tendon properties, and therefore we hypothesized that the whole human patellar tendon and its distinct collagen fibrils would display similar mechanical properties. Human patellar tendons ($n = 5$) were mechanically tested in vivo by ultrasonography. Biopsies were obtained from each tendon, and individual collagen fibrils were dissected and tested mechanically by atomic force microscopy. The Young's modulus was 2.0 ± 0.5 GPa, and the toe region reached 3.3 ± 1.9% strain in whole patellar tendons. Based on dry cross-sectional area, the Young's modulus of isolated collagen fibrils was 2.8 ± 0.3 GPa, and the toe region reached 0.86 ± 0.08% strain. The measured fibril modulus was insufficient to account for the modulus of the tendon in vivo when fibril content in the tendon was accounted for. Thus, our original hypothesis was not supported, although the in vitro fibril modulus corresponded well with reported in vitro tendon values. This correspondence together with the fibril modulus not being greater than that of tendon supports that fibrillar rather than interfibrillar properties govern the subfailure tendon response, making the fibrillar level a meaningful target of intervention. The lower modulus found in vitro suggests a possible adverse effect of removing the tissue from its natural environment. In addition to the primary work comparing the two hierarchical levels, we also verified the existence of viscoelastic behavior in isolated human collagen fibrils.

atomic force microscopy; collagen; fibril dimensions; modulus; toe region

TENDON TISSUE PLAYS AN ESSENTIAL role in transmitting contractile forces to bone to generate movement and is therefore uniquely designed to resist sizeable loads (up to ~8 times body wt) during human locomotion (16, 22). However, despite this inherent quality, both overuse injuries and complete tendon ruptures occur. The precise mechanism(s) for tendon injuries remains unknown, but it is possible that there are one or more "weak links" in the tendon structure (36).

Address for reprint requests and other correspondence: R. B. Svensson, Institute of Sports Medicine Copenhagen, Bispebjerg Hospital, Bldg. 8, 1. Floor, Bispebjerg Bakke 23, 2400 Copenhagen NV, Denmark (e-mail: svensson.nano@gmail.com).

Tendon is regarded a biological composite with collagen fibrils embedded in a ground substance of primarily proteoglycans and water (45). The collagen fibril is considered the basic force-transmitting unit of tendon, although its specific importance compared with other matrix components is yet to be firmly established (41, 42, 44, 45). Fibrils are made up of tropocollagen molecules arranged in a quarter-staggered manner as described by the Hodge-Petruska model (43) and are held together by intermolecular cross-links. However, exact knowledge of how forces are transferred through the tendon structure remains to be determined. It has been suggested that fibrils are continuous throughout the length of the tendon (13, 44), which would imply similar strains at the fibril and tendon level. On the other hand, other results support a discontinuous fibril model, in which case force transfer must occur between neighboring fibrils (19, 38, 45). Discontinuous fibrils would allow the strain of tendons to exceed that of the lower levels of the hierarchy (19) and enable fibril stiffness to exceed tendon stiffness. If fibrils are much stiffer than tendons then the majority of deformation takes place between fibrils, and fibril quality becomes less important for the overall tendon response than the quality of the interfibrillar matrix. In contrast, if fibrils have similar stiffness to tendons, interfibrillar deformation is small, and the quality of fibrils dominates tendon properties.

Few available studies have attempted to directly compare tendon mechanical properties at different hierarchical levels, and, to the best of our knowledge, none have done so in a human model. Sasaki and Odajima (48) reported the tangent modulus of the collagen molecule > fibril > tendon. In contrast, An et al. (1) summarized mechanical data from the existing literature and showed the modulus of procollagen molecules < collagen fiber < collagen fascicle < tendon. These conflicting observations leave questions regarding the mechanical properties of individual structural levels of tendon and the force transmission between these levels unanswered. Previous attempts to compare different hierarchical levels of tendon may have been hampered due to distinctions between phenotype, species, age, gender, and loading history of the examined tendons (4) in addition to methodological issues of mechanical testing (9).

Ultrasonography-based measurement of tendon properties has proven an attractive noninvasive technique of assessing human whole tendon behavior in vivo (32, 34, 35). This methodology has allowed for characterization of in vivo human patellar tendon mechanical properties (26), and the technique has been widely applied to examine tendon adaptation to aging

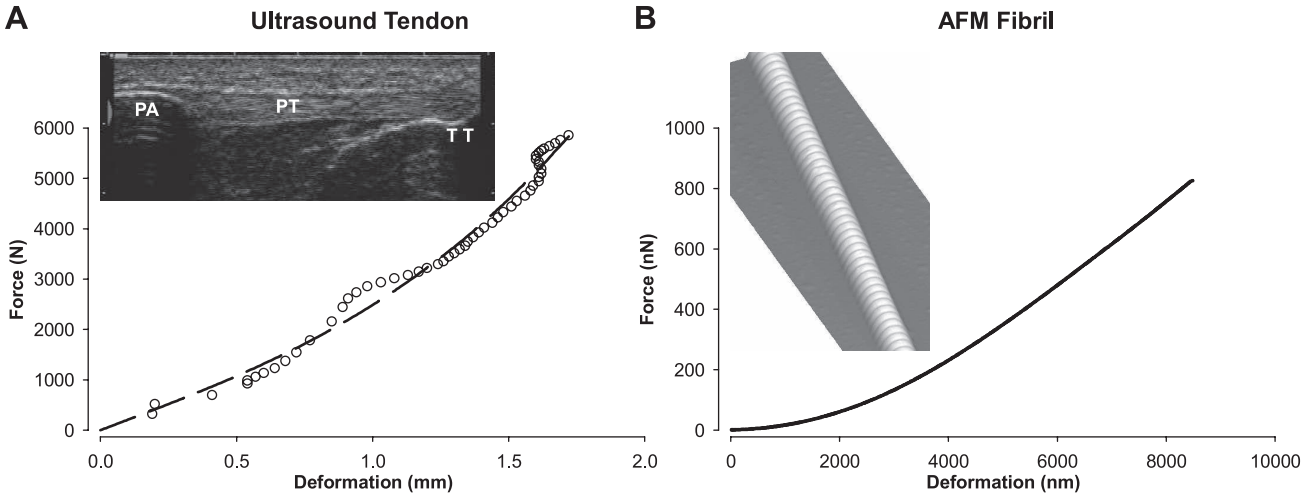

Fig. 1. Representative graphs illustrating force-deformation data for a patellar tendon and fibril. *A*: force-deformation data obtained by ultrasonography on a human patellar tendon (for clarity, only every 3rd point is displayed). *Inset* shows untrasound image used for determining deformation. The following three points of interest are indicated: the patella (PA), patellar tendon (PT), and tibial tuberosity (TT). Data were fitted to a 3rd-order polynomial (black dashed line). *B*: force-deformation data from a patellar tendon fibril obtained by atomic force microscopy (AFM). *Inset* shows a three-dimensional AFM height image of the fibril with the characteristic banding pattern. The graph represents actual data points without a fit.

and habitual loading among others (28, 33, 39, 47). For ex vivo testing of human tendon substructures, microtensile devices have been applied to describe the behavior of tendon fascicles (29, 58). Tests at the fibril level have recently also become possible using, for example, atomic force microscopy (AFM) to measure the mechanical properties of individual collagen fibrils by various experimental approaches (55, 57, 60).

To date, no studies have attempted to compare in vivo whole tendon properties with properties of lower-level hierarchical structures within the same individual. In the present study, we applied the AFM and ultrasonography methodologies to investigate and compare the hierarchical mechanical properties of *1*) whole patellar tendon in vivo and *2*) isolated collagen fibrils in vitro from the same healthy human subjects. We hypothesized that the two distinct structural levels would display similar mechanical properties.

MATERIALS AND METHODS

Subjects

Five males (age: 32 ± 7 yr; weight: 90 ± 11 kg; height: 183 ± 6 cm; body mass index: 26.7 kg/m^2) participated in the study. Subjects were scheduled for elective reconstructive surgery of the anterior cruciate ligament (ACL) and were otherwise healthy. At the time of elective surgery, which was 4–6 mo postinjury, the patients had normal range of knee joint motion, no joint swelling, and were not impaired during normal activities of daily living but were unable to participate in sports activities due to knee instability. Before surgery, they underwent rehabilitation to restore normal thigh strength, and therefore the tendons did not suffer from disuse. All subjects gave their informed consent before inclusion in the study. Approval of the study was obtained from the local Ethics Committee.

In Vivo Tendon Testing

Tendon mechanics. All measurements were performed less than one month before ACL reconstruction. Subjects were seated in a custom-made rigid chair with both hips and knees flexed to an angle of 90°. A load cell (Bofors KRG-4; Bofors) was connected perpendicularly to the lower leg 1–2 cm above the medial malleolus via a leg cuff and a rigid steel rod. An ultrasound probe was fitted into a custom-made case and secured to the skin above the patellar tendon in the sagittal plane. The ultrasound probe was positioned such that the patella apex, the patellar tendon, and the tibial tuberosity were all visible within the viewing field throughout the ramp contractions (Fig. 1). Synchronous sampling of ultrasound video images and force was obtained by using a custom-built trigger device (7). The subjects performed four to five slow isometric knee extension ramps by applying gradually increasing force up to their maximum over a 10-s period. All measurements were performed on the injured side knee. Ultrasound video was recorded at 50 Hz using frame-by-frame capture software (G400-TV; Matrox Marvel, Dorval, Canada). Force was also sampled at 50 Hz, and the force signal was low pass filtered at a 1.0-Hz cutoff frequency using a fourth-order zero-lag Butterworth filter. Tendon deformation was defined as the change in distance between the patellar apex and the tibia. The deformation was measured by custom tracking software implementing the Lucas-Kanade algorithm, which has been validated previously (26, 35).

Tendon dimensions. Patellar tendon cross-sectional area (CSA) and length were determined by magnetic resonance imaging (MRI) (General Electric, Sigma Horizon LX 1.5 Tesla, T1 weighted SE) (Fig. 2), as previously described (33). In brief, tendon CSA was measured by axial-plane MRI perpendicular to the tendon at the proximal (just

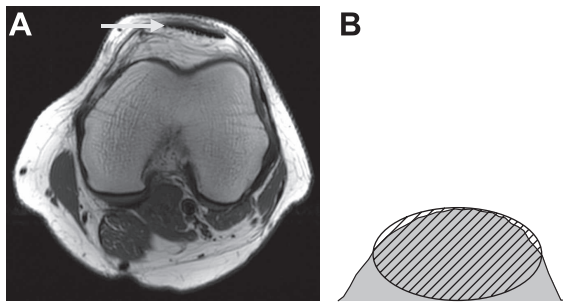

Fig. 2. *A*: axial magnetic resonance imaging of the human patellar tendon (arrow). Patellar tendon cross-sectional area was determined from axial images while tendon length was measured from similar images obtained by sagittal plane scans. *B*: fibril cross section and illustration of the two methods for determining cross-sectional area. The gray area is obtained by integrating the entire cross section, whereas the slashed ellipse is formed with one axis equal to the height and the other equal to the width at half the height.

distal to the patellar bone), mid, and distal (just proximal to the tibial tuberosity) parts of the tendon, and the average value was used for stress calculation. Reproducibility data showed that the typical error percent of repeated measures of tendon CSA was 2.5%. Patellar tendon length was determined from sagittal plane MRI as the distance from the dorsal insertion at the patella apex to the dorsal insertion on the tibia.

Tendon biopsies. During ACL reconstructive surgery, a small tendon sample was taken from the patellar tendon ACL graft of each patient. A thin tendon fiber bundle containing ~10 fascicles was obtained from the anterior aspect and mid one-third of the tendon. The biopsies were then wrapped in sterile gauze moistened by 0.15 M phosphate-buffered saline (PBS) and stored at −20°C. Storage at −20°C in PBS has been reported not to affect mechanical properties (23), which is in agreement with our own unpublished data on fascicles.

Single Collagen Fibril Testing

Sample preparation. Mechanical testing of collagen fibrils (Fig. 1) was performed using a recently described method (55). Two fibrils were tested from each subject. Briefly, small droplets of epoxy glue (DANA LIM Blå Epoxy 335) were deposited ~200 μm apart on a secluded dry collagen fibril (Fig. 3) and cured overnight. The dry fibril was imaged by tapping-mode AFM to determine CSA and ensure structural integrity. One glue droplet was then detached from the substrate using a sharp AFM tip. The detached glue patch was attached with fresh epoxy to another AFM cantilever ($k_{spring} \sim 0.42$ N/m) in such a way that the fibril was sandwiched between the cantilever and the glue patch. The epoxy cured overnight before the fibril was mechanically tested in 0.15 M PBS using a PicoForce AFM scanner (55).

Fibril mechanics. Collagen fibril testing was performed by continuously ramping the sample-cantilever distance. The ramp distance is the sum of fibril deformation and cantilever bending. Fibril deformation was targeted at 4% strain, and cantilever bending was assumed to be 1 μm when selecting the ramp distance. Because actual cantilever bending differed from 1 μm, peak strains also differ from 4%. Data were acquired in a piecewise manner by physically moving the detector as previously described (55). For this method to work, it is necessary that a mechanical equilibrium is reached, which was achieved by continuous ramping for at least 1 min before starting data acquisition. For repeated measurements within an experiment, the modulus had a coefficient of variation below 2%.

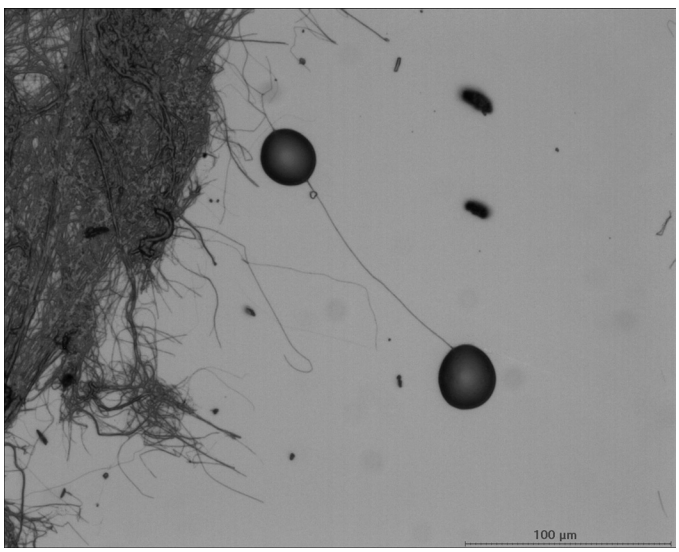

Fig. 3. Optical image of a secluded fibril from a human patellar tendon. The fibril has been glued to the surface by two glue droplets placed ~ 200 μm apart.

Viscoelasticity. To verify the effect of strain rate that we previously reported, mechanical tests were made at different strain rates (9.81, 19.6, 39.2, 78.5, 157, and 314 μm/s), and a stepwise stress relaxation test ("0" μm/s) was also performed as described previously (55). The order in which strain rates were applied varied between experiments. Only the fibril test at 9.81 μm/s was used for comparison with whole tendon properties, since this strain rate (~5%/s) corresponded most closely to that of the in vivo tendon test (~0.6%/s).

Fibril dimensions. The length of fibril between the two initial glue droplets was measured by optical microscopy. In addition, the distance moved with the AFM in the z direction to stretch the fibril was determined. The two measures were in good agreement, and the average value was used (mean difference = 3.25 μm). CSA was determined from AFM images. Side angles in AFM cross sections of fibrils were often smaller than expected for tip convolution, and fibril flattening was observed. For this reason, fibril CSA was calculated as the average of *1*) the integrated area under the fibril contour and *2*) the area of an ellipse with one diameter equal to the fibril height and the other equal to the width at half the height (Fig. 2). *Method 1* yielded CSA 20% larger than *method 2*.

Biochemical Analyses

Measurements of collagen and collagen cross-link concentrations were performed as previously reported (27). Briefly, the collagen specific amino acid, hydroxyproline, was measured spectrophotometrically (14) and used for calculating the amount of collagen protein and expressed as a fraction of the dry mass (wt/wt). Hydroxylysylpyridinoline (HP), lysylpyridinoline (LP), and pentosidine (PENT) cross-links of collagen were separated via a single reversed-phase high-performance liquid chromatography (HPLC) run (3) and detected by their natural fluorescence. The HPLC determination of cross-link concentrations in the samples was based on the use of pure HP, LP, and PENT compounds with known concentrations as external standards. The concentrations of the cross-links are expressed as mole per mole of collagen.

Data Reduction and Statistical Analysis

Hierarchy comparison. Ultrasound tendon stress-strain data were analyzed to a greatest common stress for each subject. To reduce noise, each curve was fitted using a third-order polynomial ($r^2 > 0.97$ in all cases) (Fig. 1). No noise was observed for fibrils; therefore, the raw data rather than a fitted curve were used. Dry fibril CSA was used for calculation of fibril stress because it is simpler to measure and is not affected by the tapping force during tapping-mode AFM imaging (see DISCUSSION for further details). Because the stress-strain relation becomes more linear at higher stress, Young's modulus was determined by linear regression to the final 20% stress for both tendons and fibrils.

To evaluate the nonlinear properties of fibrils compared with whole tendon, the length of the toe region was evaluated by extrapolating the linear region onto the strain axis:

$$\text{toe length} = \varepsilon - \left(\sigma / E\right)$$

where ϵ and σ are the maximal strain and stress, respectively, and E is the modulus. Two-tailed Student's paired t-tests were used to examine if fibril and whole tendon mechanical parameters differed. An α level of 0.05 was considered significant. Results are reported as group means ± SD unless otherwise stated.

Fibril viscoelasticity. The effect of strain rate on fibril modulus was analyzed as previously reported (55) by subtracting the stepwise stress-relaxation curve from the dynamic curves to obtain the viscous component of the response. The force onset moved to higher strain with increased strain rate and time. The residual strain responsible for the shift in onset probably represents an increased molecular align-

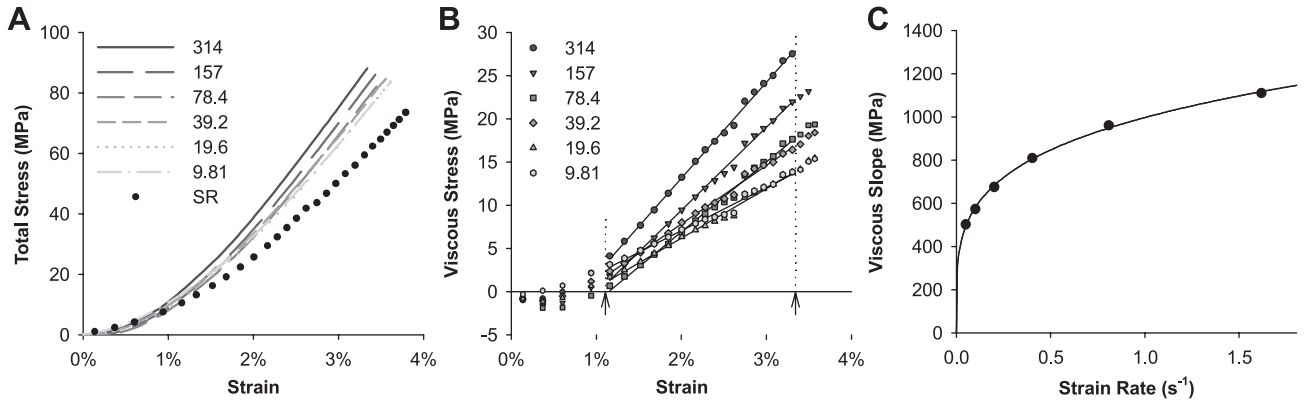

Fig. 4. Example of single fibril viscoelasticity analysis. *A*: stress-strain response of a single fibril loaded dynamically at rates from 9.81 to 314 μm/s and a "zero" rate by stepwise stress relaxation (SR). *B*: viscous stress-strain response obtained by subtracting SR data from the dynamic data. Linear fits made in the range indicated by arrows are shown as black lines. *C*: slope of the linear fits plotted against strain rate. The data are fitted with a power function (black line).

ment. We used the onset of the stepwise stress-relaxation curve for all curves in each experiment and thereby maintained their relative shifts. Because the viscous component becomes negative in the regions of residual strain, we only made linear regression within the strain range where all curves demonstrated positive viscous components (Fig. 4*B*).

RESULTS

Mechanical Characteristics

The main focus of this study was to compare mechanical properties at the fibril and whole tendon hierarchical levels. In Table 1, the sample characteristics at each level of the hierarchy are summarized. The measured values of modulus and toe length are shown in Fig. 5. The mean value of the modulus was 2.0 ± 0.5 GPa for the whole tendon and 2.8 ± 0.3 GPa for the fibril. The mean length of the toe region was 3.3 ± 1.9% for tendons and 0.86 ± 0.08% for fibrils.

Correlating the modulus of fibrils with that of their parent tendons, there was a tendency for increased fibril modulus with increasing tendon modulus albeit the correlation failed to reach significance ($r^2 = 0.59$, $P = 0.13$). There was no correlation between toe region length at the fibril and tendon levels ($r^2 = 0.01$, $P = 0.87$). The absolute modulus at the two hierarchical levels is not directly comparable; see the DISCUSSION for details.

Fibril testing achieved 2.5% lower maximal strain than the whole tendon because of limitations in maximum measurable force with our current AFM setup. However, the toe region at the fibril level was 2.4% shorter than at the tendon level ($P = 0.04$). Subtracting the toe region from the maximum strain, the length of the linear region was similar at the two levels, namely 2.8% for tendons and 2.7% for fibrils.

Table 1. *Structural and mechanical properties*

	Tendon In Vivo	Fibril In Vitro
Length	44 ± 4 mm	200 ± 10 μm
Cross-sectional area	97 ± 10 mm^2	14000 ± 4000 nm^2
Maximum test force	5.6 ± 0.6 kN	1.1 ± 0.3 μN
Maximum test stress	54 ± 9 MPa	76 ± 11 MPa
Maximum test deformation	2.7 ± 0.7 mm	7.0 ± 0.7 μm
Maximum test strain	6.1 ± 1.5%	3.6 ± 0.3%

Values are means ± SD. For fibrils, the length is the tested rather than total length. For fibrils, dry cross-sectional area is reported.

Although the tested fibril length was only ~200 μm, the visible length of fibrils was often >500 μm, and, on occasion, fibrils could be followed for up to 1 mm in the optical microscope. We never observed any split or fused fibrils.

Effect of Strain Rate

The Young's modulus for fibrils increased with rising deformation rate (Fig. 4*A*), and the viscous component shows a linear strain dependency (Fig. 4*B*). We also observe that the slope of the viscous component vs. strain (η) increased with strain rate (ν) following a power function (Fig. 4*C*), in agreement with our previous findings (55).

$$\eta = a \times \nu^b$$

The parameters of the power function were determined by a repeated-measures linear ANOVA on log(η) vs. log(ν) with the testing order as covariate. The effect of order was not significant ($P = 0.90$), but the rate effect was highly significant ($P < 0.001$) with $a = 710$ (600–840) MPa·s^b and $b = 0.23$ (0.22–0.24) [mean (95% confidence interval)]. The b value below one is in agreement with the behavior we previously reported indicating shear-thinning properties (55).

Biochemical Results

The mean collagen content was 64 ± 7% of the dry mass. The mean content of cross-links in the tendons were as follows: HP: 0.81 ± 0.23 mol/mol, LP: 0.020 ± 0.006 mol/mol, and PENT: 0.022 ± 0.008 mol/mol. There was a strong positive correlation between PENT and age ($r^2 = 0.91$, $P = 0.01$). Neither HP, LP, nor PENT correlated significantly with Young's modulus or toe length at either the tendon or the fibril level.

DISCUSSION

Young's Modulus

Hierarchical comparison. To compare fibrils and native tendons, it is necessary to determine how much of the tendon is actually made up of fibrils, e.g., identifying the effective CSA (Fig. 6). One way to do this would be to assume that the fraction is equal to the mass fraction of collagen, which is 64% of the total dry mass, which in turn is ~35% of the native

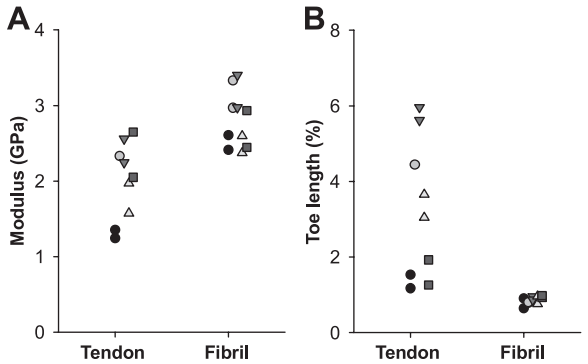

Fig. 5. Measured values of modulus (*A*) and toe region length (*B*) at the tendon and fibril levels. Data points with the same style are from the same subject. Data points are shifted along the *x*-axis for clarity.

hydrated tendon mass (10, 56). This gives a total dry collagen content in native tendon of 22%, and, assuming that fibrils are the only major tensile-bearing units, a fibril Young's modulus of 2.8 GPa using dry CSA would predict a tendon Young's modulus of 0.6 GPa. Another approach would be to account for the volume fraction of hydrated fibrils in the tendon and the fibril swelling upon hydration. Volume fraction assessed by electron microscopy is ~60% (27). Reported values of fibril swelling vary depending on measuring method. AFM measurements have generally found swelling of 50–100% in fibril diameter (24, 30, 57), whereas X-ray methods have found values of 30–40% (37, 49). This approach would predict a tendon Young's modulus in the range 0.4–1.0 GPa depending on the magnitude of swelling.

The cause of the difference in swelling between AFM and X-ray measurements is unknown. It is possible that swelling in AFM is affected by surface proteoglycans; however, in a small pilot study on chondroitinase-ABC-treated fibrils, we saw no significant reduction in swelling. We observed that dry fibrils are flattened onto the substrate surface, and, upon hydration, this flattening may disappear. This would cause an additional increase in fibril height, leading to an overestimated swelling since the height is generally used to measure sizes in AFM due to tip convolution in the sample plane. Although the exact reason for the difference in swelling is unknown, it is our opinion that overestimation of fibril swelling in AFM is more likely than underestimation with the X-ray method, especially when the intention is to measure swelling in the bulk tendon.

Regardless of the method chosen, it is clear that the measured fibril Young's modulus, when adjusted for hydration and volume fraction, predicts much lower tendon Young's modulus than the 2.0 GPa that was measured (Fig. 6). Here the ~40% volume fraction of extrafibrillar matrix was assumed to not contribute to the tendon modulus, which we believe is a reasonable assumption. If the extrafibrillar matrix was to account for the difference in modulus between tendon and fibrils, it should have a modulus of 1.8–4 GPa (by the rule of mixtures), which is unreasonably high.

Methodological considerations. It is interesting to notice that the tendon Young's modulus predicted from the fibril Young's modulus falls in the same range as most in vitro studies of human patellar tendon, which ranges from 0.3 to 1 GPa (2, 9, 11, 29). By comparison, in vivo studies similar to the present work have generally yielded greater modulus values in the range of 0.8–2.2 GPa (6, 12, 40, 47). For the in vitro moduli, technical issues with gripping can cause an underestimated modulus; however, studies gripping on the natural bone insertions and measuring local deformation in the central part, thus largely precluding the gripping issues, still find moduli far below 2 GPa (2, 9). Gripping is also an issue in the fibril measurements, and preliminary results (data not shown) using fibrils of varying length suggest that the modulus is underestimated by ~15%, which is insufficient to account for the observed difference. For the in vivo measurements, an overestimated modulus could arise from underestimating the CSA, and our preliminary work indicates that this may occur if the surrounding areas have high MRI intensity, but this is not the case for human patellar tendon. Accounting for these technical issues may reduce the gap between in vivo and in vitro results but cannot explain the entire difference. This indicates that removing the tendon from its native environment reduces the modulus, even at the fibril level. The nature of this effect is unknown but could be related to interruption of lateral force transmission between collagen molecules (50). It has been reported that tendon has a lower hydration in vivo than in physiological saline in vitro (10, 56), and this could affect mechanical properties. In a recent study, we did not find any influence of environment ionic composition on fibril modulus, suggesting that it may be the change in hydration per se that is responsible for the reduced modulus in vitro (54). An adverse effect of hydration could have implications for optimal handling of tendon grafts as well as tendon injuries where swelling is present.

Other studies have investigated fibril mechanical properties using a range of techniques and tissues, and their findings are partially summarized in Table 2. The present results are the highest reported modulus values from direct measurements, and, as such, there are no current results that are capable of explaining the large stiffness of human patellar tendon in vivo. In Table 2, only the indirect measurements from Brillouin scattering and molecular modeling are in a range

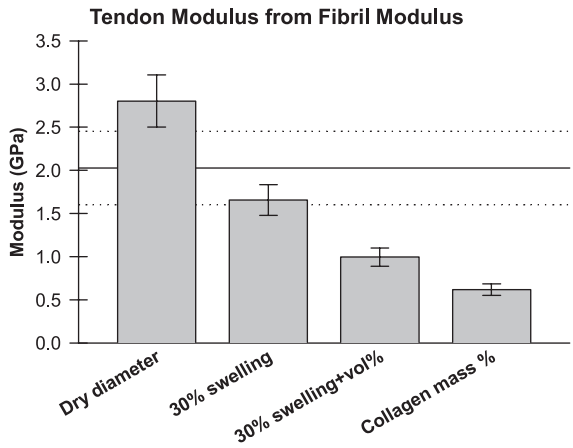

Fig. 6. Comparing modulus at the fibril and tendon level. The bars show the mean modulus of fibrils using the dry diameter, as it would be using a 30% swelled fibril diameter (30% swelling), the predicted tendon modulus using the volume fraction in addition to 30% swelling (30% swelling + vol%), and the predicted tendon modulus using instead the ratio of dry collagen mass to native tendon mass (Collagen mass%). Error bars: 95% confidence intervals. Solid horizontal line is the measured in vivo tendon modulus, and dashed lines are 95% confidence intervals.

Table 2. *Overview of reported fibril Young's moduli*

	Tissue	State	Modulus, GPa	Reference No.
Direct methods				
AFM tensile	Human patellar tendon	PBS immersed	2.8 ± 0.34	Present study
AFM tensile	Bovine achilles	PBS immersed	0.2–0.8	57
MEMS tensile	Sea cucumber dermis	Humid (31–60%)	0.86 ± 0.45 (1.39 ± 0.73)[a]	51
AFM bending	Bovine achilles	PBS immersed	0.07–0.17	59
Indirect methods				
X-ray diffraction	Mineralized turkey tendon	Partially hydrated	0.8–3.4 (0.12–0.52)[b]	25
X-ray diffraction	Bovine achilles	0.15 M NaCl	0.43[c]	48
Brillouin scattering	Rat tail tendon	Partially hydrated	5.1	15
Modeling methods				
Molecular model	None	Fully hydrated	4.36[d]	8
Molecular model	None	Fully hydrated	0.3–1.2[e]	21

AFM, atomic force microscopy; MEMS, micro-electro-mechanical system. [a]Value using a 27% swelling in diameter. In parenthesis is the value using dry diameter. [b]Hydration and volume fraction accounted for. In parenthesis is the "nonmineralized" value. [c]Hydration and volume fraction accounted for. Fibrils from specimen with 0.4 GPa modulus in vitro. [d]Hydration accounted for. A modulus of 38 GPa was predicted beyond ~30% strain. [e]A newer and more advanced model by the same group as the one above.

that could fit the measured tendon modulus, and both techniques evaluate mechanical properties at higher strain rates. Due to viscoelastic behavior of collagen fibrils as shown in the present work and that of indirect (15) and modeling (20) methods, the modulus determined at such high strain rates would be overestimated compared with the fibril and tendon measurements in the present study. In addition, new modeling results using more advanced methods have yielded lower modulus values (Table 2).

Toe Length

It is worth mentioning that, during daily walking activity, the human patellar tendon likely operates in the toe region of the stress-strain curve. Previous studies have described the human knee extensor forces during walking and small-amplitude hopping (5, 17). From these studies, patellar tendon stress during walking would be in the range of 5–15 MPa assuming a tendon CSA of 100 mm^2, which is a reasonable estimate for an average human male (Table 1) (40). During high-intensity jumping, the tendon can reach ~ 40 MPa (16). For comparison, the tendon stress at the end of the toe region was 10 ± 6 MPa in the present work, indicating that tendon operates near the end of the toe region during normal ambulation and operates in the linear region during running and jumping activities. The toe region at the fibril level was significantly shorter than at the tendon level, which is in agreement with X-ray measurements (48) and supports the common belief that the tendon toe region originates in unfolding of macroscopic waviness (crimping) in tendon fiber bundles (31). Crimping can give rise to kinks at the fibril level (18, 46), but we observed no such kinks in the fibrils tested here, possibly because of stretching during sample preparation.

Biochemistry

There was no correlation between any of the measured cross-links and modulus at either the fibril or tendon level. This suggests that even the lower cross-link densities are sufficient to avoid molecular slippage within the tested mechanical range such that additional cross-links have little or no further effect. However, the cross-link density may still affect the maximal stress that can be achieved before fibrils start yielding by molecular slippage (8). To investigate this, testing the fibrils and tendons to failure would be necessary, which was not possible in the present work. At the fibril level, an additional potential problem is the time requirement of our single fibril technique, which limits the sample size. This is a problem when comparing with a parameter like cross-linking, which is measured in the bulk and likely covers individual fibrils with a range of cross-link concentrations.

Limitations

There are some inherent shortcomings to the present method. First, for technical reasons, the lowest strain rate used in fibril testing was 10-fold higher than for tendons. From the power function for the viscous stress (see RESULTS), we predict that fibrils at a strain rate of 0.5%/s would have 0.15 GPa lower Young's modulus than at 5%/s. This difference is rather small and would only strengthen our conclusions. Second, the lack of statistically significant results for correlation between cross-link concentration and mechanical properties may be explained by the limited sample size due to the unique nature of our material. Third, the period of dehydration required while the epoxy cures could increase the modulus by increased cross-linking (52); however, this does not explain why fibril modulus is too low to account for tendon modulus. Finally, we observed a bias toward large-diameter fibrils because only those visible

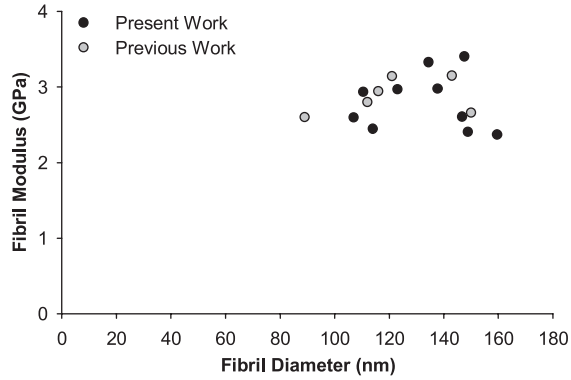

Fig. 7. Relationship between fibril modulus and diameter. Black dots are data from the present work, and gray dots are data from a previous publication (54) also tested in 150 mM PBS at 9.81 μm/s deformation rate. Diameters were backcalculated from cross-sectional areas assuming circularity.

in the optical microscope could be isolated for testing in the AFM. The tested fibrils had a mean dry diameter of 133 nm, equivalent to a hydrated diameter of ~170 nm (assuming 30% swelling), which is much larger than the <100-nm mean diameter observed by electron microscopy on human patellar tendons (27, 53). The tested fibrils may therefore not be fully representative of the fibril population. To our knowledge, there are no reports suggesting a negative correlation between fibril diameter and modulus; in fact, it has been proposed that large-diameter fibrils may demonstrate an increased modulus (41). In addition, we have not observed a relationship between fibril diameter and modulus in any of our works using the present method (Fig. 7). Thus, there is little evidence to suggest that the bias in fibril diameter would explain the low fibril modulus.

In conclusion, in this work, we present the first within-subject study of the mechanical properties of the human tendon hierarchical structure at the fibril and tendon level. Our initial hypothesis that fibril stress-strain properties directly govern overall tendon mechanical properties could not be supported by the present data. Data showed that the modulus of individual fibrils (2.8 GPa), when corrected for hydration and volume fraction (~1 GPa), was insufficient to account for the Young's modulus of their parent tendons in vivo (2.0 GPa). This finding is difficult to reconcile in the absence of other major tendon components of greater stiffness, which suggests a possible loss of stiffness in ex vivo testing. That the loss of stiffness is apparently present in both tissue and fibrils indicates that fibrils govern tissue properties. Finally, our results confirm the presence of viscoelastic and shear thinning behavior at the fibril level.

ACKNOWLEDGMENTS

R. B. Svensson, P. Hansen: Conception and design, experimental work, data analysis and interpretation, manuscript preparation. T. Hassenkam, B. T. Haraldsson, M. Krosgaard, M. Kjaer: Conception and design, manuscript editing and revision. P. Aagaard: Conception and design, data analysis, manuscript editing and revision. V. Kovanen: Experimental work, data analysis, manuscript editing and revision. S. P. Magnusson: Conception and design, data analysis and interpretation, manuscript editing and revision.

GRANTS

The study was supported by the Danish Agency for Science Technology and Innovation Grant 271-08-0384 (S. P. Magnusson)

DISCLOSURES

All authors declare no potential conflicts of interest.

REFERENCES

1. **An KN, Sun YL, Luo ZP.** Flexibility of type I collagen and mechanical property of connective tissue. *Biorheology* 41: 239–246, 2004.
2. **Atkinson TS, Ewers BJ, Haut RC.** The tensile and stress relaxation responses of human patellar tendon varies with specimen cross-sectional area. *J Biomech* 32: 907–914, 1999.
3. **Bank RA, Beekman B, Verzijl N, de Roos JA, Sakkee AN, TeKoppele JM.** Sensitive fluorimetric quantitation of pyridinium and pentosidine crosslinks in biological samples in a single high-performance liquid chromatographic run. *J Chromatogr B Biomed Sci App* 703: 37–44, 1997.
4. **Bennett MB, Ker RF, Dimery NJ, Alexander RM.** Mechanical properties of various mammalian tendons. *J Zool* 209: 537–548, 1986.
5. **Besier TF, Fredericson M, Gold GE, Beaupre GS, Delp SL.** Knee muscle forces during walking and running in patellofemoral pain patients and pain-free controls. *J Biomech* 42: 898–905, 2009.
6. **Bojsen-Moller J, Brogaard K, Have MJ, Stryger HP, Kjaer M, Aagaard P, Magnusson SP.** Passive knee joint range of motion is unrelated to the mechanical properties of the patellar tendon. *Scand J Med Sci Sports* 17: 415–421, 2007.
7. **Bojsen-Moller J, Hansen P, Aagaard P, Kjaer M, Magnusson SP.** Measuring mechanical properties of the vastus lateralis tendon-aponeurosis complex in vivo by ultrasound imaging. *Scand J Med Sci Sports* 13: 259–265, 2003.
8. **Buehler MJ.** Nanomechanics of collagen fibrils under varying cross-link densities: Atomistic and continuum studies. *J Mech Behav Biomed Mater* 1: 59–67, 2008.
9. **Butler DL, Grood ES, Noyes FR, Zernicke RF, Brackett K.** Effects of structure and strain-measurement technique on the material properties of young human tendons and fascia. *J Biomech* 17: 579–596, 1984.
10. **Chimich D, Shrive N, Frank C, Marchuk L, Bray R.** Water-content alters viscoelastic behavior of the normal adolescent rabbit medial collateral ligament. *J Biomech* 25: 831–837, 1992.
11. **Chun KJ, Butler DL.** Spatial variation in material properties in fascicle-bone units from human patellar tendon. In: *Experimental Mechanics in Nano and Biotechnology*, edited by Lee S, Kim Y. Stafa-Zurich, Switzerland: Trans Tech Publications, 2006, p. 797–802.
12. **Couppe C, Hansen P, Kongsgaard M, Kovanen V, Suetta C, Aagaard P, Kjaer M, Magnusson SP.** Mechanical properties and collagen cross-linking of the patellar tendon in old and young men. *J Appl Physiol* 107: 880–886, 2009.
13. **Craig AS, Birtles MJ, Conway JF, Parry DAD.** An estimate of the mean length of collagen fibrils in rat tail-tendon as a function of age. *Connect Tissue Res* 19: 51–62, 1989.
14. **Creemers LB, Jansen DC, van Veen-Reurings A, van den Bos T, Everts V.** Microassay for the assessment of low levels of hydroxyproline. *Biotechniques* 22: 656–658, 1997.
15. **Cusack S, Miller A.** Determination of the elastic constants of collagen by brillouin light scattering. *J Mol Biol* 135: 39–51, 1979.
16. **Finni T, Komi PV, Lepola V.** In vivo human triceps surae and quadriceps femoris muscle function in a squat jump and counter movement jump. *Eur J Appl Physiol* 83: 416–426, 2000.
17. **Finni T, Komi PV, Lepola V.** In vivo muscle mechanics during locomotion depend on movement amplitude and contraction intensity. *Eur J Appl Physiol* 85: 170–176, 2001.
18. **Franchi M, Fini M, Quaranta M, De Pasquale V, Raspanti M, Giavaresi G, Ottani V, Ruggeri A.** Crimp morphology in relaxed and stretched rat achilles tendon. *J Anat* 210: 1–7, 2007.
19. **Fratzl P, Misof K, Zizak I, Rapp G, Amenitsch H, Bernstorff S.** Fibrillar structure and mechanical properties of collagen. *J Struct Biol* 122: 119–122, 1998.
20. **Gautieri A, Buehler MJ, Redaelli A.** Deformation rate controls elasticity and unfolding pathway of single tropocollagen molecules. *J Mech Behav Biomed Mater* 2: 130–137, 2009.
21. **Gautieri A, Vesentini S, Redaelli A, Buehler MJ.** Hierarchical structure and nanomechanics of collagen microfibrils from the atomistic scale up. *Nano Lett* 11: 757–766, 2011.
22. **Giddings VL, Beaupre GS, Whalen RT, Carter DR.** Calcaneal loading during walking and running. *Med Sci Sports Exerc* 32: 627–634, 2000.
23. **Goh KL, Chen Y, Chou SM, Listrat A, Bechet D, Wess TJ.** Effects of frozen storage temperature on the elasticity of tendons from a small murine model. *Animal* 4: 1613–1617, 2010.
24. **Grant CA, Brockwell DJ, Radford SE, Thomson NH.** Effects of hydration on the mechanical response of individual collagen fibrils (Abstract). *Appl Phys Lett* 92: 3902, 2008.
25. **Gupta HS, Messmer P, Roschger P, Bernstorff S, Klaushofer K, Fratzl P.** Synchrotron diffraction study of deformation mechanisms in mineralized tendon. *Phys Rev Lett* 93: 158101, 2004.
26. **Hansen P, Bojsen-Moller J, Aagaard P, Kjaer M, Magnusson SP.** Mechanical properties of the human patellar tendon, in vivo. *Clin Biomech* 21: 54–58, 2006.
27. **Hansen P, Haraldsson BT, Aagaard P, Kovanen V, Avery NC, Qvortrup K, Larsen JO, Krogsgaard M, Kjaer M, Magnusson SP.** Lower strength of the human posterior patellar tendon seems unrelated to mature collagen cross-linking and fibril morphology. *J Appl Physiol* 108: 47–52, 2010.
28. **Hansen P, Aagaard P, Kjaer M, Larsson B, Magnusson SP.** Effect of habitual running on human achilles tendon load-deformation properties and cross-sectional area. *J Appl Physiol* 95: 2375–2380, 2003.
29. **Haraldsson BT, Aagaard P, Krogsgaard M, Alkjaer T, Kjaer M, Magnusson SP.** Region-specific mechanical properties of the human patella tendon. *J Appl Physiol* 98: 1006–1012, 2005.

30. **Heim AJ, Koob TJ, Matthews WG.** Low strain nanomechanics of collagen fibrils. *Biomacromolecules* 8: 3298–3301, 2007.
31. **Jarvinen TAH, Jarvinen TLN, Kannus BB, Jozsa L, Jarvinen M.** Collagen fibres of the spontaneously ruptured human tendons display decreased thickness and crimp angle. *J Orthop Res* 22: 1303–1309, 2004.
32. **Kjaer M, Langberg H, Bojsen-Moller J, Koskinen SO, Mackey A, Heinemeier K, Holm L, Skovgaard D, Dossing S, Hansen M, Hansen P, Haraldsson B, Caroe I, Magnusson SP.** Novel methods for tendon investigations. *Disabil Rehabil* 30: 1514–1522, 2008.
33. **Kongsgaard M, Reitelseder S, Pedersen TG, Holm L, Aagaard P, Kjaer M, Magnusson SP.** Region specific patellar tendon hypertrophy in humans following resistance training. *Acta Physiol* 191: 111–121, 2007.
34. **Maganaris CN, Paul JP.** In vivo human tendon mechanical properties. *J Physiol (Lond)* 521: 307–313, 1999.
35. **Magnusson SP, Hansen P, Aagaard P, Brond J, Dyhre-Poulsen P, Bojsen-Moller J, Kjaer M.** Differential strain patterns of the human gastrocnemius aponeurosis and free tendon, in vivo. *Acta Physiol Scand* 177: 185–195, 2003.
36. **Magnusson SP, Langberg H, Kjaer M.** The pathogenesis of tendinopathy: balancing the response to loading. *Nat Rev Rheumatol* 6: 262–268, 2010.
37. **Meek KM, Fullwood NJ, Cooke PH, Elliott GF, Maurice DM, Quantock AJ, Wall RS, Worthington CR.** Synchrotron X-ray diffraction studies of the cornea, with implications for stromal hydration. *Biophys J* 60: 467–474, 1991.
38. **Mosler E, Folkhard W, Knorzer E, Nemetschekgansler H, Nemetschek T, Koch MHJ.** Stress-induced molecular rearrangement in tendon collagen. *J Mol Biol* 182: 589–596, 1985.
39. **Narici MV, Maganaris CN.** Adaptability of elderly human muscles and tendons to increased loading. *J Anat* 208: 433–443, 2006.
40. **Onambele GNL, Burgess K, Pearson SJ.** Gender-specific in vivo measurement of the structural and mechanical properties of the human patellar tendon. *J Orthop Res* 25: 1635–1642, 2007.
41. **Parry DAD.** The molecular and fibrillar structure of collagen and its relationship to the mechanical properties of connective tissue. *Biophys Chem* 29: 195–209, 1988.
42. **Parry DAD, Barnes GRG, Craig AS.** A comparison of size distribution of collagen fibrils in connective tissues as a function of age and a possible relation between fibril size distribution and mechanical properties. *Proc R Soc Lond B Biol Sci* 203: 305–321, 1978.
43. **Petruska JA, Hodge AJ.** A subunit model for tropocollagen macromolecule. *Proc Natl Acad Sci USA* 51: 871–876, 1964.
44. **Provenzano PP, Vanderby R.** Collagen fibril morphology and organization: Implications for force transmission in ligament and tendon. *Matrix Biol* 25: 71–84, 2006.
45. **Puxkandl R, Zizak I, Paris O, Keckes J, Tesch W, Bernstorff S, Purslow P, Fratzl P.** Viscoelastic properties of collagen: Synchrotron radiation investigations and structural model. *Philos Trans R Soc Lond B Biol Sci* 357: 191–197, 2002.
46. **Raspanti M, Manelli A, Franchi M, Ruggeri A.** The 3D structure of crimps in the rat achilles tendon. *Matrix Biol* 24: 503–507, 2005.
47. **Reeves ND, Maganaris CN, Narici MV.** Effect of strength training on human patella tendon mechanical properties of older individuals. *J Physiol (Lond)* 548: 971–981, 2003.
48. **Sasaki N, Odajima S.** Elongation mechanism of collagen fibrils and force-strain relations of tendon at each level of structural hierarchy. *J Biomech* 29: 1131–1136, 1996.
49. **Sasaki N, Shiwa S, Yagihara S, Hikichi K.** X-ray-diffraction studies on the structure of hydrated collagen. *Biopolymers* 22: 2539–2547, 1983.
50. **Screen HRC, Chhaya VH, Greenwald SE, Bader DL, Lee DA, Shelton JC.** The influence of swelling and matrix degradation on the microstructural integrity of tendon. *Acta Biomater* 2: 505–513, 2006.
51. **Shen ZL, Dodge MR, Kahn H, Ballarini R, Eppell SJ.** Stress-strain experiments on individual collagen fibrils. *Biophys J* 95: 3956–3963, 2008.
52. **Silver FH, Christiansen DL, Snowhill PB, Chen Y.** Role of storage on changes in the mechanical properties of tendon and self-assembled collagen fibers. *Connect Tissue Res* 41: 155–164, 2000.
53. **Svensson M, Movin T, Rostgard-Christensen L, Blomen E, Hultenby K, Kartus J.** Ultrastructural collagen fibril alterations in the patellar tendon 6 years after harvesting its central third. *Am J Sports Med* 35: 301–306, 2007.
54. **Svensson RB, Hassenkam T, Grant CA, Magnusson SP.** Tensile properties of human collagen fibrils and fascicles are insensitive to environmental salts. *Biophys J* 99: 4020–4027, 2010.
55. **Svensson RB, Hassenkam T, Hansen P, Magnusson SP.** Viscoelastic behavior of discrete human collagen fibrils. *J Mech Behav Biomed Mater* 3: 112–115, 2010.
56. **Thornton GM, Shrive NG, Frank CB.** Altering ligament water content affects ligament pre-stress and creep behaviour. *J Orthop Res* 19: 845–851, 2001.
57. **van der Rijt JAJ, van der Werf KO, Bennink ML, Dijkstra PJ, Feijen J.** Micromechanical testing of individual collagen fibrils. *Macromol Biosci* 6: 697–702, 2006.
58. **Yamamoto E, Hayashi K, Yamamoto N.** Mechanical properties of collagen fascicles from stress-shielded patellar tendons in the rabbit. *Clin Biomech* 14: 418–425, 1999.
59. **Yang L, van der Werf KO, Fitié CFC, Bennink ML, Dijkstra PJ, Feijen J.** Mechanical properties of native and cross-linked type I collagen fibrils. *Biophys J* 94: 2204–2211, 2008.
60. **Yang L, van der Werf KO, Koopman B, Subramaniam V, Bennink ML, Dijkstra PJ, Feijen J.** Micromechanical bending of single collagen fibrils using atomic force microscopy. *J Biomed Mater Res A* 82A: 160–168, 2007.